Title	Ambipolar Carrier Mobility in Binary Blend Thin Film of Non-Peripheral Alkylphthalocyanines
Author(s)	Fujii, Akihiko; Nakano, Shohei; Fukui, Hitoshi et al.
Citation	Journal of Physics: Conference Series. 2016, 704, p. 012006-012006
Version Type	VoR
URL	https://hdl.handle.net/11094/75679
rights	Content from this work may be used under the terms of the Creative Commons Attribution 3.0 licence. Any further distribution of this work must maintain attribution to the author(s) and the title of the work, journal citation and DOI.
Note	

PAPER • OPEN ACCESS

Ambipolar Carrier Mobility in Binary Blend Thin Film of Non-Peripheral Alkylphthalocyanines

To cite this article: Akihiko Fujii *et al* 2016 *J. Phys.: Conf. Ser.* **704** 012006

View the article online for updates and enhancements.

Related content

- FTIR spectroscopy of conformational probes introduced into binary blends of polymers
D I Kamalova, L R Abdrazakova and S N Naumova

- Fast Ambipolar Carrier Transport and Easy Homeotropic Alignment in a Metal-Free Phthalocyanine Derivative
Hiroaki Iino, Yukiko Takayashiki, Jun-ichi Hanna et al.

- Suppression of the Drift Field in the p-Type Quasineutral Region of a Semiconductor p—n Junction
Cai Xue-Yuan, Yang Jian-Hong and Wei Ying

Recent citations

- Selective crystal growth in bar-coating process of polymorphic pentyl-substituted phthalocyanine thin film
Mitsuhiro Nakatani *et al*

- Miscibility and carrier transport properties in binary blend system of non-peripherally octa-hexyl-substituted phthalocyanine analogues
Dai Nakagawa *et al*

- Glass-sandwich-type organic solar cells utilizing liquid crystalline phthalocyanine
Toshiki Usui *et al*

Ambipolar Carrier Mobility in Binary Blend Thin Film of Non-Peripheral Alkylphthalocyanines

Akihiko Fujii[1], Shohei Nakano[1], Hitoshi Fukui[1], Takashi Saito[1], Masashi Ohmori[1], Yo Shimizu[2], and Masanori Ozaki[1]

[1]Division of Electrical, Electronic and Information Engineering, Graduate School of Engineering, Osaka University, Suita, Osaka 565-0871, Japan
[2]Synthetic Nano-Function Materials Group, Research Institute for Ubiquitous Energy Devices, Kansai Center, National Institute of Advanced Industrial Science and Technology (AIST), Ikeda, Osaka 563-8577, Japan

E-mail: afujii@eei.eng.osaka-u.ac.jp

Abstract. Charge carrier mobility in blend films of two types of soluble phthalocyanine derivatives with different substituent length, 1,4,8,11,15,18,22,25-octapentyl-phthalocyanine (C5PcH$_2$) and 1,4,8,11,15,18,22,25-octahexyl-phthalocyanine (C6PcH$_2$) has been investigated. The charge carrier mobility was measured by the time-of-flight technique. In the case of C5PcH$_2$ blend ratio below 25 mol%, the high mobility, such as 0.8-1.1 cm^{2}V^{-1}s^{-1} for hole and 0.6 cm^{2}V^{-1}s^{-1} for electron, were obtained at room temperature. In the thin films with C5PcH$_2$ above 30 mol%, the charge carrier mobility decreased by one order of magnitude and had the different temperature dependence from that below 25 mol%. The marked change of the charge carrier mobility depending on the blend ratio of phthalocyanine derivatives has been discussed by taking the miscibility and the molecular packing structure into consideration.

1. Introduction

Organic electronics is one of the most attractive and important research fields to realize light-weight, flexible and ubiquitous electronic devices in commercial base. In particular, a recent trend of this research field is "printed electronics" based on a solution processing, and realization of the low-cost organic thin film devices, such as organic light-emitting diodes, organic field effect transistors and organic photovoltaics, is promising. Required characteristics of organic semiconductors available for the printed electronics are high solubility in common organic solvents, spontaneous molecular alignment during the solvent evaporation to form a high quality thin film on a substrate, and high carrier mobility, and so on. Some organic semiconductor materials, such as pentacene derivatives [1,2], benzothienobenzothiophene derivatives [3] and dinaphthothienothiophene derivatives [4], were reported and must be the candidates applicable to the printed electronics.

   Recently, we reported unique properties of a phthalocyanine derivateive, 1,4,8,11,15,18,22,25-octahexylphthalocyanine (C6PcH$_2$) [5]. C6PcH$_2$ is soluble in common organic solvents and has the discotic liquid crystalline (LC) properties. C6PcH$_2$ forms a hexagonal columnar structure by self-organization in the LC and crystal phases, and demonstrates the high ambipolar carrier mobility comparable to that of amorphous silicon, 1.08 and 0.43 cm^{2}V^{-1}s^{-1} for hole and electron at room temperature, respectively. C6PcH$_2$ is available for bulk-heterojunction (BHJ) solar cells as a donor

material and the high power conversion efficiency (PCE) of 3.2 % [6,7] were reported. In the $C6PcH_2$ based BHJ solar cells, the PCE could be improved to be 3.8% [8] using the blend donor materials of $C6PcH_2$ and its analogue molecule, 1,4,8,11,15,18,22,25- octapentylphthalocyanine ($C5PcH_2$).

Utilizing the mixture of small molecules with different alkyl-substituents, improvement of charge carrier mobility, and molecular alignment control have been reported [9-11]. The details of fundamental properties of the blend thin film of $C5PcH_2$ and $C6PcH_2$ should include an important essence to realize high performance devices, however, have not been clarified yet.

In this study, the charge carrier mobility in the blend films of $C5PcH_2$ and $C6PcH_2$ was investigated by a time-of-flight technique and discussed by taking the miscibility and molecular packing structure in the films.
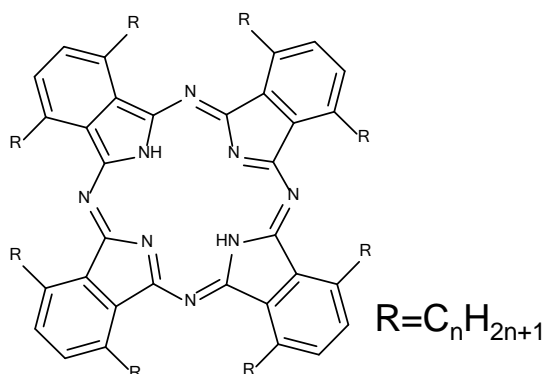

Figure 1. Molecular structures of $C5PcH_2$ (n=5) and $C6PcH_2$ (n=6).

2. Experimental

The molecular structures of $C5PcH_2$ and $C6PcH_2$ are shown in Fig. 1. $C5PcH_2$ and $C6PcH_2$ were synthesized according to the literature [12] with slight modifications, and fully purified by column chromatography (silica-gel with toluene as eluent) followed by repetitive recrystallization from toluene-methanol (1:2) solution.

The mixtures of $C5PcH_2$ and $C6PcH_2$ were prepared by the following procedures. $C5PcH_2$ and $C6PcH_2$ were dissolved in toluene, and toluene was vaporized under a N_2 atmosphere. The molar ratios of $C5PcH_2$ and $C6PcH_2$ were 12.5:87.5, 25:75, 30:70, 37.5:62.5, 50:50 and 75:25.

A sandwich cell, consisting of two indium tin oxide (ITO)-coated glass substrates and a 9-μm-thick PET spacer, was used for the TOF measurements. The actual cell gap was evaluated by an interference technique of light transmittance. The mixture of $C5PcH_2$ and $C6PcH_2$ was heated to a temperature in the isotropic phase for injecting into the cell by a capillary action, and cooled down to room temperature in a vacuum.

The cell was set onto a sample stage with a heater, which could control the sample temperature during the measurement by TOF technique, in a vacuum chamber. A DC bias voltage was applied between the electrodes using batteries connected in series and the sample was irradiated with a Nd:YAG pulsed laser (λ: 355 nm, pulsed width: 1 ns). The generated transient current was detected by an oscilloscope (LeCroy HDO 4054), which allowed the transit time to be determined, and the mobility μ was estimated according to the equation, $\mu = l^2/V\tau$, where l, V, and τ are the sample thickness, applied voltage and transit time, respectively.

The phase transition behavior of the mixtures of $C5PcH_2$ and $C6PcH_2$ was investigated by differential scanning calorimetry (DSC, TA instruments Q2000) and polarizing optical microscopy (POM, Nikon ECLIPSE E600 POL) equipped with a Mettler FP82HT Hot Stage and Mettler FP90 Central Processor.

X-ray diffraction (XRD) pattern was measured using an X-ray diffractometer (Rigaku RINT 2000) with Cu Kα line. A measured sample was prepared by separating the pair of glass substrates of the

sandwich cell. The lattice parameter d was calculated from the XRD patterns using Bragg's law; $n\lambda = 2d\sin\theta$, where n is an integer, λ is the X-ray wavelength of 1.5418 Å, and θ is the Bragg angle.

3. Results and Discussion

In order to confirm the miscibility of $C5PcH_2$ and $C6PcH_2$, the thermal properties in the mixture of $C5PcH_2$ and $C6PcH_2$ were investigated. Figure 2 shows the phase transition diagram determined by using the DSC and POM of the mixture of $C5PcH_2$ and $C6PcH_2$. A LC phase appears between 161 °C and 169 °C for $C6PcH_2$, while no LC phase exists in the case of $C5PcH_2$. The clearing points of the mixtures were kept constant in the case of $C5PcH_2$ blend ratio lower than 50 mol%. The melting points almost coincided with Le Chatelier-Schröder relation [13-15] exhibited as a theoretical thermal behavior of the melting point for each blend ratio. The eutectic point of the mixture could be approximately determined to be 20 mol% of the $C5PcH_2$ blend ratio from the calculation using Le Chatelier-Schröder relation. Therefore, these results indicate that the mixtures of $C5PcH_2$ and $C6PcH_2$ possess the miscibility, and each compound is mixed in the molecular level.
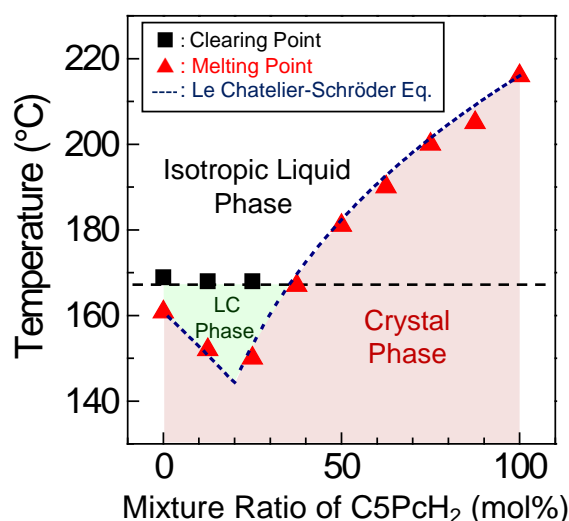

Figure 2. Phase transition diagram for the mixtures of $C5PcH_2:C6PcH_2$.

Figure 3 shows typical decay curves of the transient photocurrents for hole and electron in the blend film of $C5PcH_2:C6PcH_2$=50:50 under an applied electric field of 27.9 kV/cm at room temperature. The decay curves with the clear kink points were observed throughout the temperature range of the crystal phase and the transit times for hole and electron transport could be determined. The decay curves of other blend ratios of $C5PcH_2$ and $C6PcH_2$ were also nondispersive behaviors except for those of the electron in the blend ratios of 30:70 and 75:25. The charge carrier mobility was independent of the applied field, which is a typical behavior observed in liquid crystalline semiconductors [16].

Figures 4(a) and 4(b) show the temperature dependence of the hole and electron mobility in the blend films of $C5PcH_2:C6PcH_2$, respectively. Comparing the temperature dependence, the obvious different behaviors could be found among the three regions, that is, in the $C5PcH_2$ blend ratio below 25 mol%, 30-37.5 mol%, and 50-75 mol%. In the region of $C5PcH_2$ blend ratio below 25 mol%, the charge carrier mobility was independent of the temperature and approximately 0.25 $cm^2V^{-1}s^{-1}$ for hole and 0.3 $cm^2V^{-1}s^{-1}$ above about 140 °C, while below about 140 °C the charge carrier mobility increased from 0.5 to 1.0 $cm^2V^{-1}s^{-1}$ for hole and from 0.3 to 0.6 $cm^2V^{-1}s^{-1}$ for electron as the temperature decreased. In the region of 30-37.5 mol%, the charge carrier mobility slightly increased from 0.01 to 0.05 $cm^2V^{-1}s^{-1}$ with decreasing the temperature. In the region of 50-75 mol%, the charge carrier mobility was independent of the temperature and approximately 0.25 $cm^2V^{-1}s^{-1}$ for hole and 0.3 $cm^2V^{-1}s^{-1}$ above about 140 °C, while below about 140 °C the charge carrier mobility increased from 0.05 to

0.1 cm^{2}V^{-1}s^{-1} with decreasing the temperature. The temperature dependence of the charge carrier mobility in crystal phase could be explained by the volume expansion of the unit lattice in the molecular packing structure. The detailed studies about the temperature dependence of the lattice parameter in the C5PcH$_2$:C6PcH$_2$ blend single crystal by using X-ray structure analysis are now in progress, and the relationship between the mobility and lattice parameter would be reported elsewhere.
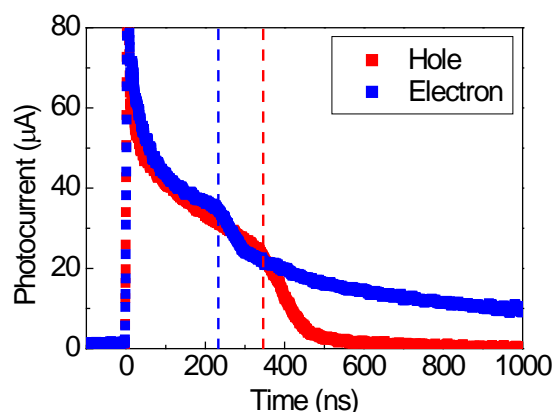

Figure 3. Transient photocurrent decay curves of the blend film of C5PcH$_2$:C6PcH$_2$=50:50 under the field of 27.9 kV/cm at room temperature.

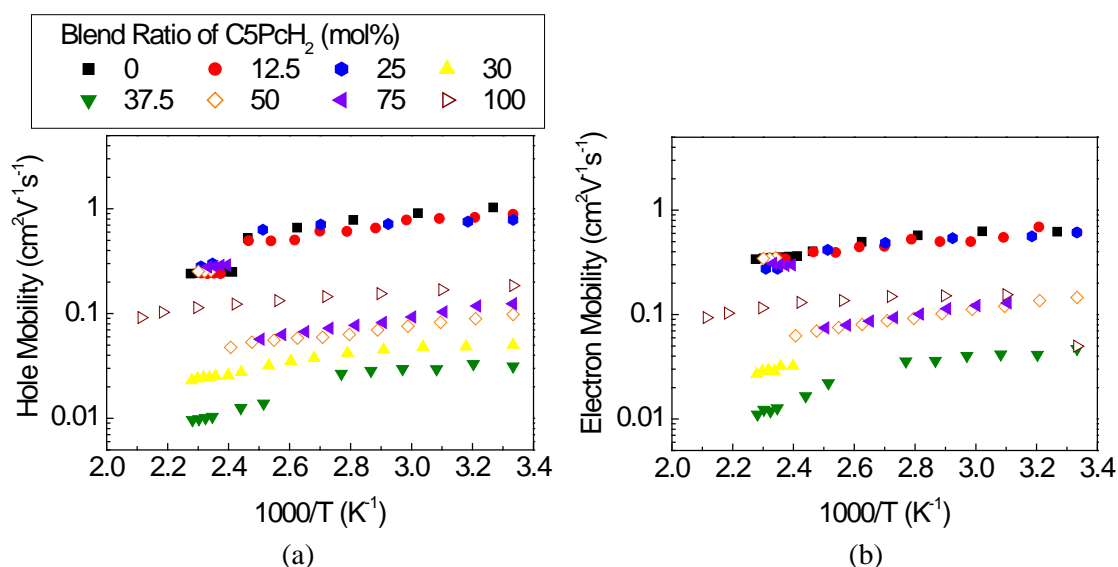(a)   (b)

Figure 4. Temperature dependence of hole mobility (a) and electron mobility (b) in the C5PcH$_2$:C6PcH$_2$ blend films.

Comparing the charge carrier mobility in the blend films of C5PcH$_2$:C6PcH$_2$, the C5PcH$_2$ blend ratio dependence of the mobility at room temperature is shown in Fig. 5. In the case of C5PcH$_2$ blend ratio below 25 mol%, both hole and electron mobilities kept high values close to those of C6PcH$_2$. The hole mobility slightly decreased from 1.1 to 0.8 cm^{2}V^{-1}s^{-1} with increasing the blend ratio of C5PcH$_2$, while the electron mobility kept constant, 0.6 cm^{2}V^{-1}s^{-1}. In the case of C5PcH$_2$ blend ratio above 30 mol%, both hole and electron mobilities markedly decreased by one order of magnitude, and the hole mobility slightly increased with increasing the blend ratio of C5PcH$_2$.

Figures 6(a) and 6(b) show the XRD patterns of the blend films with C5PcH$_2$:C6PcH$_2$ and the magnified figure in the range of 2θ=4-6°, respectively. In the case of C5PcH$_2$ blend ratio below 25

mol%, the diffraction peaks at 4.86° and 26.02° appeared, which correspond to the $d(100)$ lattice parameter of hexagonal column formed by $C6PcH_2$ (Fig. 7(a)) and the $d(001)$ lattice parameter of inter-molecular distance, respectively. It is considered that the molecular packing structure like $C6PcH_2$ was formed and the molecules were stacked in order, since $C6PcH_2$ was dominant for the self-organization in the appearance of the liquid crystal phase in the $C5PcH_2$ blend ratio below 25 mol%, therefore, the charge carrier mobility was kept high.
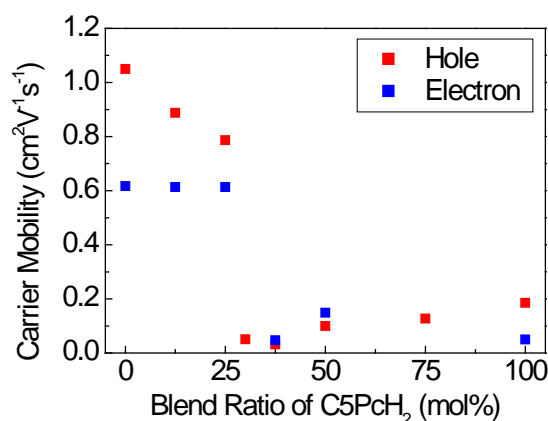

Figure 5. $C5PcH_2$ blend ratio dependence of charge carrier mobility in the $C5PcH_2$:$C6PcH_2$ blend films at room temperature.
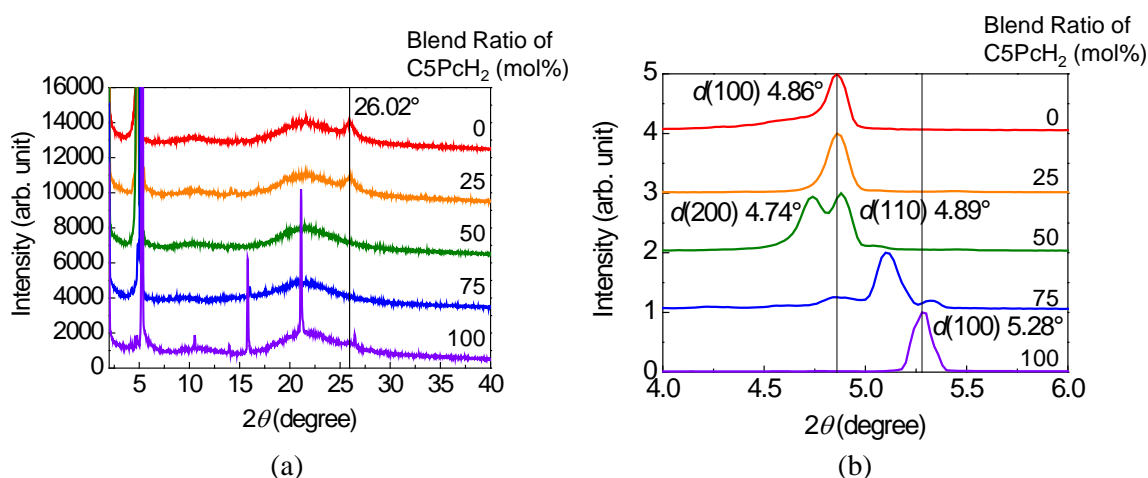

(a)   (b)

Figure 6. XRD patterns of the $C5PcH_2$:$C6PcH_2$ blend films at room temperature in the angle ranges of 2-40° (a) and 4-6° (b).

In the $C5PcH_2$ blend ratio of 50 mol%, the two diffraction peaks at 4.74° and 4.89° were observed, which correspond to the $d(200)$ and $d(110)$ lattice parameter of rectangular column (Fig. 7 (b)). It is supposed that the lattice constant in the a-axis direction of rectangular lattice became longer, while that in the b-axis direction became shorter, because equivalent mixing caused the distortion of the hexagonal lattice.

In the case of $C5PcH_2$ blend ratio above 50 mol%, the diffraction peak shifted from 4.89° to 5.28° corresponding to the $d(100)$ in Fig. 7(a) as the blend ratio of $C5PcH_2$ increased. It is considered that the mean length of the alkyl chains around the column became shorter with increasing the blend ratio of $C5PcH_2$, because of short substituent of $C5PcH_2$, resulting in the decrease of the inter-columnar distance.

The diffraction peaks around 26°, which originates from the molecular stacking, however, disappeared in the higher $C5PcH_2$ blend ratio than 25 mol%, therefore, the marked decrease of the carrier mobility in the film with $C5PcH_2$ above 30 mol% must be explained by the disordered stacking in the columnar structure. Since the inter-molecular overlapping of π-orbitals must strongly contribute to the carrier transport, therefore, it is considered that the carrier transport in the blend film of $C5PcH_2$ and $C6PcH_2$ should be dominated by the order of molecular packing like π-stacking rather than the lattice parameter like inter-columnar distance.
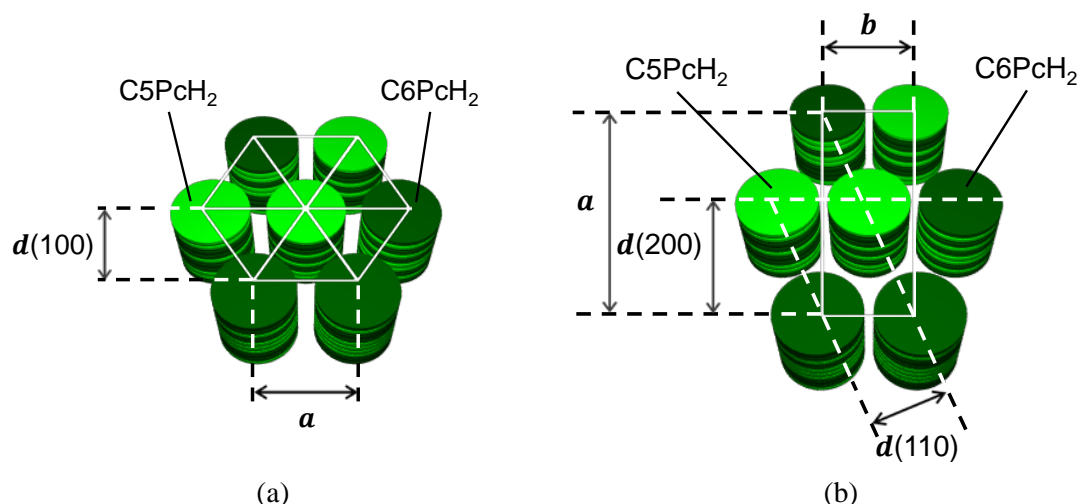

(a)   (b)

Figure 7. Schematic diagrams of (a) hexagonal and (b) rectangular columnar structures in the blend films of $C5PcH_2$:$C6PcH_2$.

4. Conclusions

The charge carrier mobility in the blend films of $C5PcH_2$ and $C6PcH_2$ were investigated. The phase diagram of the mixture of $C5PcH_2$ and $C6PcH_2$ was determined from the thermal properties, it was found that the mixture possess the miscibility. In the case of $C5PcH_2$ blend ratio below 25 mol%, both hole and electron mobilities were kept high values comparable with those of $C6PcH_2$, while both hole and electron mobilities markedly decreased by one order of magnitude in the case of $C5PcH_2$ blend ratio above 30 mol%. From the results of XRD measurement, the molecular structure of the mixture film obviously changed depending on the blend ratio of $C5PcH_2$, that must be strongly related with the behavior of the charge carrier transport.

References

[1] Chang J, Sakanoue T, Olivier Y, Uemura T, Dufourg-Madec M, Yeates S G, Cornil J, Takeya J, Troisi A and Sirringhaus H 2011 *Phys. Rev. Lett.* **107** 066601
[2] Llorenete G R, Dufourg-Madec M, Crouch D J, Printchard R G, Ogier S and Yeates S G 2009 *Chem. Commun.* 3059
[3] Uemura T, Hirose Y, Uno M, Takimiya K and Takeya J 2009 *Appl. Phys. Express* **2** 111501

[4]   Nakayama K, Hirose Y, Soeda J, Yoshizumi M, Uemura T, Uno M, Li W, Kang M J, Yamagishi M, Okada Y, Miyazaki E, Nakazawa Y, Nakao A, Takimiya K and Takeya J 2011 *Adv. Mater.* **23** 1626

[5]   Miyake Y, Shiraiwa Y, Okada K, Monobe H, Hori T, Yamasaki N, Yoshida H, Cook M J, Fujii A, Ozaki M and Shimizu Y 2011 *Appl. Phys. Express* **4** 021604

[6]   Hori T, Miyake Y, Yamasaki N, Yoshida H, Fujii A, Shimizu Y and Ozaki M 2010 *Appl. Phys. Express* **3** 101602

[7]   Hori T, Fukuoka N, Masuda T, Miyake Y, Yoshida H, Fujii A, Shimizu Y and Ozaki M 2011 *Sol. Energy Mater. Sol. Cells* **95** 3087

[8]   Fukui H, Nakano S, Uno T, Dao Q, Saito T, Fujii A, Shimizu Y and Ozaki M 2014 *Org. Electron.* **15** 1189

[9]   Wegewijs B R and Siebbeles L D A 2002 Phys. Rev. B **65** 245112

[10] Shimizu Y, Matsuda Y, Nekelson F, Miyake Y, Yoshida H, Fujii A and Ozaki M 2009 *Proc. of SPIE* **8279** 82790G

[11] G. Schweicher, G. Gbabode, F. Quist, O. Debever, N. Dumont, S. Sergeyev and Y. H. Geerts: 2009 *Chem. Mater.* **21** 5867

[12] Swarts J C, Langner E H G, Krokeide-Hove N and Cook M J 2001 *J. Mater. Chem.* **11** 434

[13] Le Chatelier H 1894 *C. R. Acad. Sci.* **118** 638

[14] Schröder I 1893 *Z. Phys. Chem.* **11** 449

[15] Van Laar J J 1903 *Arch. Neerl.* **8** 264

[16] Yoshino K, Nakayama H, Ozaki M, Onoda M and Hamaguchi M 1997 *Jpn. J. Appl. Phys.* **36** 5183